Quantifying the σ and π interactions between U(V) f orbitals and halide, alkyl, alkoxide, amide and ketimide ligands

Wayne W. Lukens,[1]* Norman M. Edelstein,[1] Nicola Magnani,[1] Trevor W. Hayton,[2]* Skye Fortier,[2] Lani A. Seaman[2]

[1]Chemical Sciences Division, Lawrence Berkeley National Lab, Berkeley, CA 94720
[2]Department of Chemistry and Biochemistry, University of California Santa Barbara, Santa Barbara, CA 93106

Corresponding Author
*email: wwlukens@lbl.gov, hayton@chem.ucsb.edu

Abstract

f Orbital bonding in actinide and lanthanide complexes is critical to their behavior in a variety of areas from separations to magnetic properties. Octahedral f^1 hexahalide complexes have been extensively used to study f orbital bonding due to their simple electronic structure and extensive spectroscopic characterization. The recent expansion of this family to include alkyl, alkoxide, amide, and ketimide ligands presents the opportunity to extend this study to a wider variety of ligands. To better understand f orbital bonding in these complexes, the existing molecular orbital (MO) model was refined to include the effect of covalency on spin orbit coupling in addition to its effect on orbital angular momentum (orbital reduction). The new MO model as well as the existing MO model and the crystal field (CF) model were applied to the octahedral f^1 complexes to determine the covalency and strengths of the σ and π bonds formed by the f orbitals. When covalency is significant, MO models more precisely determined the strengths of the bonds derived from the f orbitals; however, when covalency was small, the CF model was better than either MO model. The covalency determined using the new MO model is in better agreement with both experiment and theory than that predicted by the existing MO model. The results emphasize the role played by the orbital energy in determining the strength and covalency of bonds formed by the f orbitals.

Introduction

Understanding the contribution of the f orbitals to bonding in actinide and lanthanide complexes is currently the subject of numerous investigations, which are aimed at addressing specific practical goals as well as exploring the fundamental behavior of f orbitals.[1-8] Among the actinides, the role of f orbitals in bonding has been extensively studied due, in part, to the desire to exploit differences in covalent bonding to separate actinides and lanthanide ions during the processing of used nuclear fuel.[9-14] This desire stems from the fact that certain lanthanides and actinides have similar ionic radii (e.g., the ionic radii of 6-coordinate Am^{3+}, Cm^{3+}, Nd^{3+}, and Pr^{3+} are 0.975 Å, 0.97 Å, 0.98 Å, and 0.99 Å, respectively) making it difficult to separate these ions based solely on differences in ionic bonding.[15] Fortunately, covalent bonding among the actinides is stronger than for the lanthanides due to the greater radial extent of the 5f orbitals relative to the 4f orbitals, which could be used as the basis for the separation of the actinides from the lanthanides.[16] Separating trivalent actinide ions with similar radii (e.g., Am^{3+} from Cm^{3+}) is more challenging and would be aided by a better understanding of covalency among actinide ions.

Given the importance that f orbitals play in bonding, this issue has been extensively studied both experimentally and computationally.[2,3,11,17-26] In general, computational studies produce a more detailed description of bonding in these systems because they can address both the strength and covalency of f orbital bonds. Experimentally determining the contributions of the f orbitals to bonding is challenging, and much of the information about the magnitude of f orbital interactions has been garnered through spectroscopic studies using crystal field models to determine the splitting of the f orbitals.[3,17-19,25,27] This approach provides useful information about the strengths of the interactions between f orbitals and ligands, but typically cannot provide detailed information about covalency. The degree of covalency in f orbital bonding is more difficult to quantify and has been studied using EPR and X-ray absorption spectroscopies.[2,26,28] The latter approach is particularly attractive since it is a general approach, which can be applied to any metal complex.

Among the most studied classes of actinide and lanthanide complexes are the octahedral hexahalide complexes (e.g., NpF_6, UF_6, $CeCl_6^{3-}$), especially those possessing a single f electron, due to the simplicity of the bonding as well as the ability to address spin-orbit coupling in a straightforward manner.[17-19,22,25,29,30] Extensive spectroscopic and computational results are available for these complexes. The octahedral, pentavalent UX_6^- complexes recently reported by us represent a unique opportunity to extend these studies from halides to a variety of ligands. These UX_6^- complexes consist of formally pentavalent uranium coordinated by alkyl (X = CH_2SiMe_3, **1**), alkoxide (X = O^{t}Bu, **2**), amide (X = NC_5H_{10}, **3**), and ketimide (X = N=C^{t}BuPh, **4**) ligands (Figure 1).[31-35] This family of complexes is ideal for studying f orbital bonding because it spans a range of commonly used ligands in organouranium chemistry, and the spectroscopic data necessary to analyze the bonding is available. Moreover, the bonding in these compounds may be compared to that in the halide complexes (X = F, Cl, Br).[17-21,36]

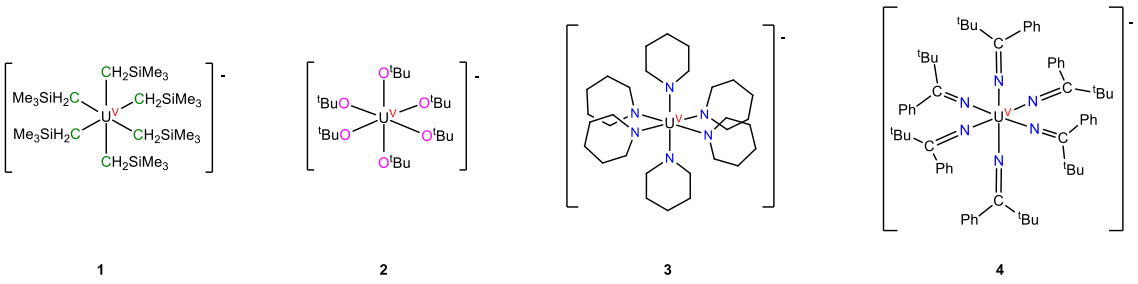

Figure 1. Structures of the non-halide octahedral U(V) complexes.

The f orbitals of an octahedral complex are split by interactions with the ligands into a non-bonding a_{2u} orbital, a π antibonding t_{2u} orbital, and a σ and π antibonding t_{1u} orbital.[17,37,38] As illustrated in Figure 2, the difference in energy between the a_{2u} and t_{2u} orbital is defined as Δ and the difference between the t_{2u} and t_{1u} orbital is defined as θ.[17,25,27] The situation is similar to the splitting of the d orbitals of an octahedral complex in that θ is roughly analogous to 10 Dq, the splitting between the t_{2g} and e_g antibonding orbitals. The most important difference between the ligand field splitting of the f orbitals and d orbitals is the presence of the non-bonding a_{2u} f orbital, which offers the potential

to determine the absolute strengths of the σ and π interactions between the f orbitals and the ligands from Δ and θ, whereas only the relative strengths of the σ and π interactions can be determined from 10 Dq. Consequently, octahedral U(V) complexes are ideal for studying π and σ bonding if Δ and θ can be determined.

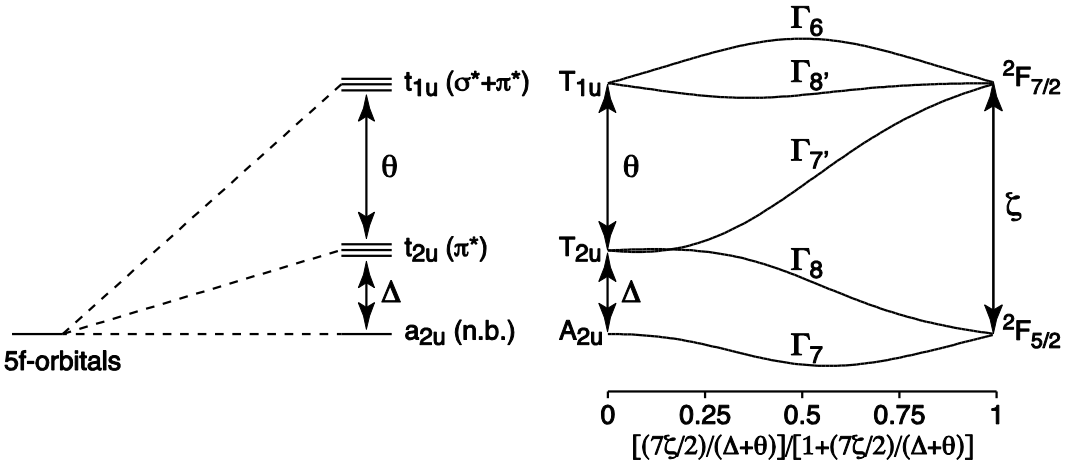

Figure 2. (left) Splitting of f orbitals in an octahedral complex showing the relationship of θ and Δ to the relative energies of the orbitals. (right) Relationship between the low-lying states of an octahedral f^1 complex as a function of the strength of the crystal field (θ and Δ) relative to spin-orbit coupling (ζ). The diagram is drawn for θ/Δ = 2 and is drawn with the barycenter of the f orbitals equal to zero.

An important factor in studying π and σ interactions in octahedral f^1 complexes is the spin-orbit (SO) coupling interaction, which is almost as strong as the ligand field in these complexes. When the orbitals (lower case) in Figure 2 are singly occupied, the resulting states (upper case) are A_{2u}, T_{1u}, and T_{2u}. As illustrated on the right side of Figure 2, SO coupling mixes these states producing a new set of states, Γ_7, Γ_8, $\Gamma_{7'}$, $\Gamma_{8'}$, and Γ_6.[17,25,27] For U(V) complexes, transitions between the these states occur in the infrared (IR) and near infrared (NIR) and are a function of the strength of ligand field, as expressed in terms of Δ, θ, and the strength of the SO coupling, ζ. As shown originally by Eisenstein and Pryce, [38] the values of Δ, θ, and ζ may be determined from a combination of spectroscopic and magnetic data using a molecular orbital (MO) model that includes

orbital reduction, which is the decrease in the orbital angular momentum of the antibonding f orbitals due to covalent bonding.[39] Subsequently, Thornley derived an MO model for octahedral f complexes that explicitly includes the effects of both overlap and covalency on orbital reduction.[37] The Eisenstein and Pryce MO model and the Thornley MO models are similar; the main difference is that orbital reduction is somewhat empirical in the Eisenstein and Pryce model while orbital reduction is a direct consequence of covalency in the Thornley model. Both the Eisenstein and Pryce and the Thornley models have been applied to a variety of f^1 complexes.[17-20]

Given the data provided by the new U(V) complexes, we attempted to find the model that best describes the experimental data and to use the parameters (Δ and θ) derived from that model to determine the strengths of the σ and π interactions between the 5f orbitals of U(V) and the ligands. To accomplish this, we modified Thornley's MO model to include the effect of covalency on spin-orbit coupling itself in addition to its effect of orbital reduction.[24,39] The model is applied to the new octahedral U(V) complexes and octahedral f^1 hexahalide complexes to determine the covalency and strengths of π and σ interactions between these ligands and the metal center. Somewhat surprisingly, all models produce very similar estimates for the strengths π and σ interactions. However, the new MO model is more precise. In addition, the amount of covalency determined using the new model is much smaller than that found by previous models.

Results and Discussion

MO model for an octahedral f^1 complex. A detailed MO model for octahedral f^1 complexes was developed by Thornley.[37] The MO-T model (Thornley's MO model) used here is identical except that the ligand s and p orbitals involved in σ bonding are hybridized prior to inclusion in the MO model.[25,37] To this model, we have included reduced spin-orbit coupling constants for the antibonding f orbitals, which were derived following the procedure used by Owen and Thornley for the d orbitals.[24] This new model will be referred to as the MO-RSO model (MO model with reduced spin orbit coupling). Reduced spin-orbit coupling has been largely ignored when analyzing bonding in actinide

and lanthanide complexes; however, its inclusion greatly affects the amount of covalency predicted by the MO models.

In the absence of SO coupling, the antibonding molecular orbitals of an f^1 complex (illustrated in Figure 3) can be described by Scheme 1 where the f' orbitals are the antibonding molecular orbitals of f parentage, the atomic f orbitals in indicated by "f", the π bonding ligand p orbitals are indicated by "x," "y," and "z," the sp hybridized ligand σ bonding orbitals are indicated by "σ," and the ligand character in the antibonding orbitals is indicated by α.[37] The numerical subscripts identify the ligands (ligands 1 and 4 lie on the x-axis, ligands 2 and 5 lie on the y-axis, and ligands 3 and 6 lie on the z-axis).[37] In Thornley's original model, the σ bonding s and p orbitals are not hybridized. However, the available spectroscopic data does not allow the effects of the ligand p and s orbitals on σ bonding to be separated, necessitating the use of a hybridized σ bonding orbital. The t_{1u} MO is both σ and π antibonding. In the t_{1u} MO, α_π is the amount of ligand character introduced by π overlap between the ligand p orbitals and the uranium f orbitals, and α_σ is the amount of ligand character due to σ overlap between the uranium f orbitals and σ bonding sp hybrid orbital. The t_{2u} MOs is π antibonding and α_π' is the amount of ligand character introduced by π overlap between the ligand p orbitals and the uranium f orbitals. The α parameters represent the unnormalized ligand character of the MOs and are identical to the metal-ligand mixing coefficients.[1,40] The normalized electron density on the ligands in the t_{1u} and t_{2u} orbitals is $N^2(\alpha_\sigma^2+\alpha_\pi^2)$ and $N'^2\alpha_\pi'^2$, respectively, where N and N' are the normalization constants. This value will be used synonymously with covalency.

a_{2u} $\quad f'_{a_2} = f_{a_2}$

$$f'_x = N\left[f_x - \tfrac{1}{2}\alpha_\pi(-x_3 - x_6 - x_2 - x_5) - \sqrt{\tfrac{1}{2}}\alpha_\sigma(-\sigma_1 - \sigma_4)\right]$$

t_{1u} $\quad f'_y = N\left[f_y - \tfrac{1}{2}\alpha_\pi(-y_1 - y_4 - y_3 - y_6) - \sqrt{\tfrac{1}{2}}\alpha_\sigma(-\sigma_2 - \sigma_5)\right]$

$$f'_z = N\left[f_z - \tfrac{1}{2}\alpha_\pi(-z_2 - z_5 - z_1 - z_4) - \sqrt{\tfrac{1}{2}}\alpha_\sigma(-\sigma_3 - \sigma_6)\right]$$

$$f'_\xi = N'\left[f_\xi - \tfrac{1}{2}\alpha'_\pi(-x_3 - x_6 + x_2 + x_5)\right]$$

t_{2u} $\quad f'_\eta = N'\left[f_\eta - \tfrac{1}{2}\alpha'_\pi(-y_1 - y_4 + y_3 + y_6)\right]$

$$f'_\zeta = N'\left[f_\zeta - \tfrac{1}{2}\alpha'_\pi(-z_2 - z_5 + z_1 + z_4)\right]$$

$$N^2 = \left(1 - 4\alpha_\pi S_\pi - 2\sqrt{2}\alpha_\sigma S_\sigma + \alpha_\pi^2 + \alpha_\sigma^2\right)^{-1}$$

$$N'^2 = \left(1 - 4\alpha'_\pi S'_\pi + \alpha'^2_\pi\right)^{-1}$$

$$NN' = \left[1 + \tfrac{1}{2}\left(-4\alpha_\pi S_\pi - 4\alpha'_\pi S'_\pi - 2\sqrt{2}\alpha_\sigma S_\sigma + \alpha_\pi^2 + \alpha'^2_\pi + \alpha_\sigma^2\right)\right]^{-1}$$

$S_\pi = \langle f_x | -x_3 \rangle$ $\qquad$ $S_\pi' = \langle f_\xi | -x_3 \rangle$ $\qquad$ $S_\sigma = \langle f_x | -\sigma_1 \rangle$

Scheme 1. Thornley's MO model[37] applied to an octahedral f^1 complex using an sp hybridized σ bonding orbital rather than separate s and p orbitals.

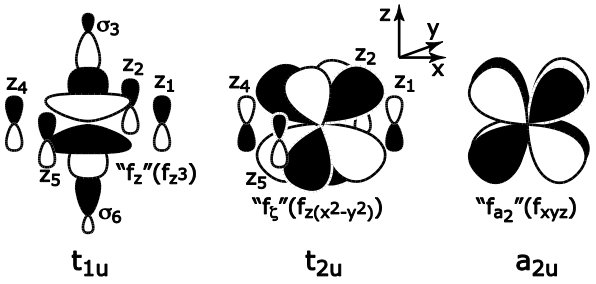

Figure 3. Antibonding MOs of an octahedral f^1 complex.

Spin-orbit (SO) coupling in these complexes is large and strongly mixes the A_{2u}, T_{2u}, and T_{1u} states when the orbitals given in Scheme 1 are populated. However, SO mixing of

these states will be smaller than that found in the free ion due to several factors. The smallest effect is caused by the involvement of the metal d and s orbitals in bonding, which will slightly screen the f orbitals and slightly decrease the SO coupling constant for the f orbitals in the complex, ζ_f, from the free ion value, $\zeta_{free\text{-}ion}$.[24] The most important effect is the Stevens' orbital reduction caused by a decrease in orbital angular momentum of the MOs due to covalent bonding.[39] For the MO given in Scheme 1, the orbital reduction factors were determined using the approach described by Thornley and are given in Scheme 2.[37]

$$k_{t_1t_1} = 1 - N^2\left[\frac{4}{3}\alpha_\pi^2 + \alpha_\sigma^2 + \frac{2\sqrt{2}}{3}\alpha_\pi\alpha_\sigma\right]$$

$$k_{t_2t_2} = 1 - 2N'^2\alpha_\pi'^2$$

$$k_{a_2t_2} = 1 - \frac{1}{2}N'^2\alpha_\pi'^2$$

$$k_{t_1t_2} = 1 - NN'\left[\frac{1}{2}\left(\alpha_\pi^2 + \alpha_\pi'^2 + \alpha_\sigma^2\right) + \sqrt{\frac{2}{15}}\alpha_\pi'\left(\alpha_\sigma - \frac{\alpha_\pi}{\sqrt{2}}\right)\right]$$

Scheme 2. Orbital reduction factors for an octahedral f^1 complex.

In addition to reducing orbital angular momentum, introduction of ligand character into the antibonding orbitals by covalent bonding has another significant impact, changing spin-orbit coupling itself, as noted by Misetich, Buch and Watson for transition metal complexes.[41,42] The origin of this effect is similar to orbital reduction: ligand character in the MOs due to covalent bonding results in SO coupling that are functions of the SO coupling constants of the ligand and metal.[24] The formulas for reduced SO coupling of an octahedral f^1 complex were determined using the approach used by Owen and Thornley for transition metal complexes.[24] These relationships are shown in Scheme 3 where ζ_f is the spin-orbit coupling constant of U(V) in the complex, and ζ_X is the atomic spin-orbit coupling of p orbital of the atom coordinated to the metal center as determined from its atomic spectrum.[43] The values of used for X = C, N, O, F, Cl, and Br are 13.5 cm^{-1}, 3 cm^{-1}, 79 cm^{-1}, 269 cm^{-1}, 588 cm^{-1}, and 2457 cm^{-1}, respectively.[43]

$$\zeta_{t_1t_1} = N^2\left[\zeta_f - \tfrac{1}{3}\left(\alpha_\pi^2 + 2\sqrt{2}\alpha_\pi\alpha_\sigma\right)\zeta_X\right]$$

$$\zeta_{t_2t_2} = N'^2\left[\zeta_f - \alpha_\pi'^2\zeta_X\right]$$

$$\zeta_{a_2t_2} = N'^2\left[\zeta_f + \tfrac{1}{2}\alpha_\pi'^2\zeta_X\right]$$

$$\zeta_{t_1t_2} = NN'\left[\zeta_f - \sqrt{\tfrac{2}{15}}\left(\alpha_\sigma\alpha_\pi' - \tfrac{\alpha_\pi\alpha_\pi'}{\sqrt{2}}\right)\zeta_X\right]$$

Scheme 3. Reduced SO coupling for an octahedral f^1 complex.

The energies and wave functions of the SO coupled 5f states (Γ_7, Γ_8, Γ_7', Γ_8', and Γ_6) can be obtained from the three energy matrices given in Scheme 4.[17,38] The SO coupled states can be expressed as mixtures of the non-relativistic states as shown in Scheme S1. The value of g for the Γ_7 ground state was originally given by Eisenstein and Pryce and is shown eqn 1 using Thornley's nomenclature for the orbital reduction parameters.[38]

Γ_7:

	A	B
A	0	$\sqrt{3}k_{a_2t_2}\zeta_{a_2t_2}$
B	$\sqrt{3}k_{a_2t_2}\zeta_{a_2t_2}$	$\Delta - \tfrac{1}{2}k_{t_2t_2}\zeta_{t_2t_2}$

Γ_8:

	C	D
C	$\Delta + \tfrac{1}{4}k_{t_2t_2}\zeta_{t_2t_2}$	$\tfrac{3}{4}\sqrt{5}k_{t_1t_2}\zeta_{t_1t_2}$
D	$\tfrac{3}{4}\sqrt{5}k_{t_1t_2}\zeta_{t_1t_2}$	$\Delta + \theta - \tfrac{3}{4}k_{t_1t_1}\zeta_{t_1t_1}$

Γ_6:

	E
E	$\Delta + \theta + \tfrac{3}{4}k_{t_1t_1}\zeta_{t_1t1}$

Scheme 4. Energy matrices for an octahedral f^1 complex

$$g(\Gamma_7) = 2\cos^2\gamma - \frac{8}{\sqrt{3}}k_{a_2t_2}\sin\gamma\cos\gamma - \frac{2}{3}\left(1 - k_{t_2t_2}\right)\sin^2\gamma \qquad (1)$$

The MO-RSO model described above cannot be used to fit the available data for octahedral f^1-complexes because as defined, it contains more parameters (α_σ^2, α_π^2, $\alpha_\pi'^2$, S_π,

S_σ, θ and Δ) than the four or five data typically available. The principal simplifying assumption is that overlap, S, is small compared to α and can be neglected. In addition to removing the overlap parameters, the number of α parameters can be decreased using the group overlaps for the σ and π interactions in the t_{1u} and t_{2u} orbitals determined from group theory by Burns and Axe.[25] The group overlap for the t_{1u} orbital is equivalent to $(2)^{1/2}$ S_σ plus $(3/2)^{1/2}$ S_π, and the group overlap for the t_{2u} orbital is $(5/2)^{1/2}$ S_π. In other words, the t_{1u} orbital participates in 2 σ and 1.5 π bonds, and the t_{2u} orbital forms 2.5 π bonds. Therefore, α_π^2 can be substituted by $(3/5)\alpha_\pi'^2$ without making any additional assumptions.[25] Using these simplifications, the MO-RSO model can be expressed using four parameters Δ, θ, $\alpha_\pi'^2$, and α_σ^2 if the values of ζ_X and ζ_f are known.

The relationship between ζ_f and the free ion value, $\zeta_{free\text{-}ion}$, must be determined before the MO-RSO model can be applied. As noted above, ζ_f should be slightly smaller than $\zeta_{free\text{-}ion}$ due to screening of the f orbitals caused by covalent bonding between the ligands and the s, p, and d orbitals of the metal center. The value of $\alpha_\pi'^2$ is particularly sensitive to ζ_f; therefore, one would like to use the spectroscopically determined value of $\alpha_\pi'^2$ to calibrate ζ_f. The only f^1 complex for which this parameter has been evaluated is NpF_6 where $\alpha_\pi'^2$ has been determined to be 0.044(3) from the degree of ^{19}F hyperfine coupling observed by EPR.[28] When the MO-RSO model is applied to NpF_6 with $\alpha_\pi'^2$ fixed at 0.044, the best fit is obtained with ζ_f = 2559 cm^{-1}. Since the calculated spin-orbit coupling constant of Np(VI) is 2666 cm^{-1},[44] $\zeta_f = 0.96\ \zeta_{free\text{-}ion}$. This relationship will be used to determine ζ_f using the calculated values of $\zeta_{free\text{-}ion}$.[44] The effect of using $\zeta_f = 0.96\ \zeta_{free\text{-}ion}$ rather than $\zeta_f = \zeta_{free\text{-}ion}$ is relatively small: the value of $\alpha_\pi'^2$ is decreased by ~0.025 and the value of Δ is decreased by ~100 cm^{-1} (Table S1). The 4% decrease in the value of ζ_f due to covalent bonding between the ligands and the s, p, and d orbitals is slightly larger than the 1.7% decrease estimated for the reduction in the 3d SO coupling in $KNiF_6$ due to covalent bonding between the ligands and the nickel s and p orbitals.[41]

In addition to the MO-RSO model, two additional models can be defined by approximating the effect of covalency on the orbital reduction factors and reduced spin

orbit coupling constants. The MO-T model is obtained when the reduced SO coupling constants are replaced by a single variable, ζ ($\zeta_{t1t1} = \zeta_{t1t2} = \zeta_{a2t2} = \zeta_{t2t2} = \zeta$ in Scheme 3), and the usual orbital reduction factors in Scheme 2 are used. The MO-T model has five parameters ($\alpha_{\pi}'^2$, α_{σ}^2, ζ, θ, and Δ). The simplest model, the crystal field (CF) model developed by Reisfeld and Crosby to analyze the spectrum of $CsUF_6$,[27] has three parameters (ζ, θ, and Δ), and is an approximation in which the reduced SO coupling constants are replaced by a single variable, ζ, as in the MO-T model and orbital reduction is not used ($k_{t1t1} = k_{t1t2} = k_{a2t2} = k_{t2t2} = 1$ in Scheme 2). As used here, "CF model" refers only to the Reisfeld and Crosby CF model.[27]

The three models are closely related and differ only in the way in which covalency affects orbital reduction and spin-orbit reduction. The CF model does not explicitly include covalency ($\alpha_{\pi}'^2 = \alpha_{\sigma}^2 = 0$), but its effects are partially accounted for by allowing ζ to vary. The MO models can be viewed as refinements of the CF model to account for the effects of covalency. In the MO-T model, the effects of covalency on orbital reduction are explicitly included, and the reduction of SO coupling by covalency is partially accounted for by allowing ζ to vary as in the CF model. In the MO-RSO model, the effects of covalency on both orbital reduction and spin orbit reduction are explicitly included.

NIR and EPR spectra of the non-halide complexes. To model the bonding in $[UX_6]^-$, the energies of the f-f transitions must be determined for **1-4.** These values are known for the halide complexes.[18,36,38,45] The NIR spectra of complexes **1-4** are shown in Figure 4 with the absorption peaks labeled by the final state. The initial state is Γ_7 all cases. The intensities of these absorption bands are weak for the alkyl, **1**, and alkoxide, **2**, complexes. The amide, **3**, and ketimide, **4**, complexes display considerably more intense absorption, which may be attributed to deviations from octahedral symmetry. In an octahedral complex, purely electronic f-f transitions are Laporte forbidden, and the observed transitions are mainly due to vibronic coupling.[27,36] Two effects can increase the intensities of these transitions, most notably deviations from octahedral symmetry, as noted by Ryan.[36] In addition, covalency can greatly increase the intensities of these

transitions through "intensity stealing".[46] In contrast to all other complexes discussed here, π bonding in **3** and **4** is anisotropic because each ligand possesses only one occupied p orbital that can act as a π donor. Because of this asymmetry in π bonding, neither complex possesses octahedral symmetry regardless of the orientations of the ligands, and more intense f-f absorption bands are possible. A similar trend in absorption intensity is observed among the halide complexes with UBr_6^- having more intense transitions than UCl_6^-, which has much intense f-f peaks than UF_6^-.[36] In this case, the increase in intensity cannot be attributed to deviations from octahedral symmetry. While $CsUF_6$ does not possess octahedral symmetry,[47] bulkier chloride and bromide ligands should enforce octahedral symmetry due to steric effects, and UF_6^- would be expected to have the strongest f-f transitions if the increase in intensity were mainly due to deviations from octahedral symmetry. Therefore, the increase in intensity for the heavier halide complexes is consistent with an increase in covalency ("intensity stealing") rather than deviation from octahedral symmetry.

Peaks assigned to the Γ_7', Γ_8', and Γ_6 states are clearly observed for all complexes except for the alkyl complex. In the alkyl complex, the energy of the Γ_6 state is not well-defined because the f-f peaks are weak and the background rises steeply due to absorptions at higher energy. The energy of Γ_6 in this case may be roughly determined from the change in the slope of the background (see SI). In the alkoxide complex, an additional feature attributable to Γ_8 is present in the NIR, while for the ketimide complex, a peak at 3240 cm^{-1} is present in the IR spectrum, and is assigned to Γ_8. In all reported octahedral U(V) complexes, the Γ_8' peak is split due to vibronic coupling, and the value of Γ_8' is determined by averaging the two features.[18,36]

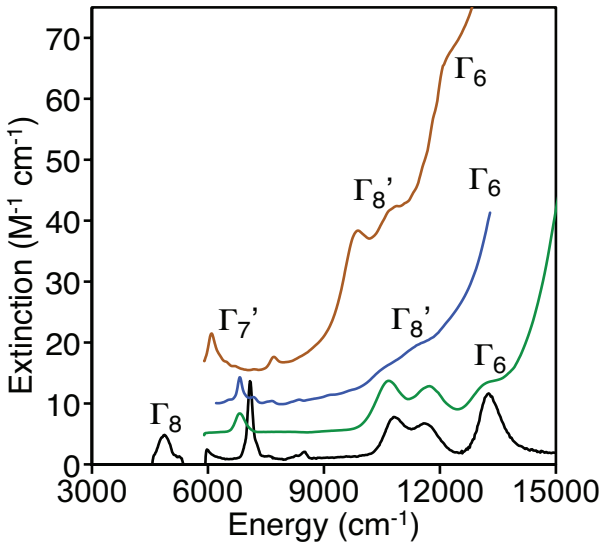

Figure 4. NIR spectra of octahedral, non-halide U(V) complexes. From top to bottom, the ligands are ketimide, **4,** (brown); alkyl, **1**, (blue); amide, **3**, (green); and alkoxide, **2**, (black). The extinction coefficients of the amide and ketimide complexes are decreased by a factor of 5 to make the plot more legible. The dip between 5500 cm^{-1} and 6000 cm^{-1} is due to solvent overtones.

In addition to the energies of the f-f transitions, the g-values determined by EPR provide additional data for analyzing the bonding in these complexes. The g-values are known for the halide complexes.[28,48-50] The EPR spectra of complexes **1**-**4** are shown in Figure 5, and their g-values are given in Table 1. Since the symmetry of these complexes is close to octahedral, one may expect their EPR spectra to consist of a single line. However, small deviations from octahedral symmetry produce slight anisotropy in the EPR spectra as previously observed for uranium halide complexes,[22,24-26] and illustrated here by the spectra of the alkyl and alkoxide complexes. One of the peaks in the spectrum of the alkoxide complex, **2**, is at too large a field to be observed with our spectrometer, and the g-value of the missing peak, 0.47, was determined by the magnetic susceptibility extrapolated to 0 K. The EPR spectrum of **2** somewhat anisotropic due to the coordination of two of the *tert*-butoxide ligands to the lithium counter ion.[32] As a result, two of the *tert*-butoxide ligands have a U-O-C angle of 140°, and only a single oxygen 2p orbital on each ligand is available to donate into the U 5f orbitals (the other 2p orbital is stabilized by interaction with the lithium cation), which makes the π bonding anisotropic

for these ligands. The other four *tert*-butoxide ligands of **2** have U-O-C angle of 167°, and the both filled oxygen 2p orbital of each ligand can interact with the uranium 5f orbitals. The spectra of both the amide and ketimide complexes are highly anisotropic due to anisotropy of π bonding in these two complexes, which is consistent with the greater intensities of the f-f transitions in the NIR as discussed above.

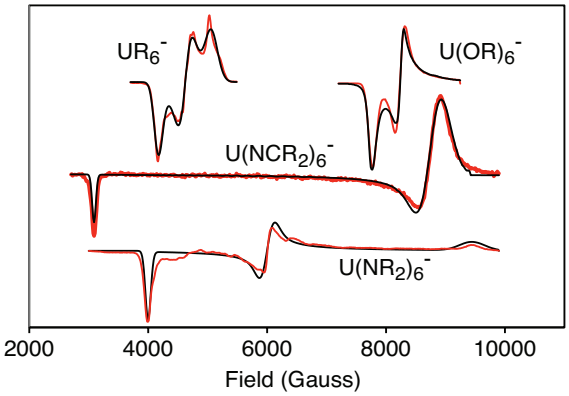

Figure 5. EPR spectra of **1-4** (red) and simulated spectra (black).

Table 1. EPR parameters for **1-4**

Compound	g_1	g_2	g_3	g_{ave}
UR_6^- (**1**)	1.58	1.42	1.30	1.43
$U(OR)_6^-$ (**2**)	0.85	0.80	0.47	0.73
$U(NR_2)_6^-$ (**3**)	1.65	1.10	0.70	1.15
$U(NCR_2)_6^-$ (**4**)	2.13	0.75	0.75	1.22

The values of the individual g-components were averaged to determine the g-value for the complex in octahedral symmetry. The EPR spectra of the halide, alkoxide, and alkyl complexes display limited anisotropy, and it is reasonable to assume that the values of the individual components may be averaged for comparison to the calculated g-value. On the other hand, the EPR spectra of **3** and **4** are highly anisotropic, and it is not obvious that averaging the g-values for these complexes is appropriate. Fortuitously, Baker and Davies have shown that a trigonal distortion of a cubic crystal field will not change the average g-value for the Γ_7 ground state.[51] The effect of such a distortion was also checked

using a crystal field model for **4**, which is trigonally distorted in the manner addressed by Baker and Davies.[35] In this case, the crystal field parameters for **4** in octahedral symmetry were transformed into C_{3v} symmetry, and a trigonal distortion was introduced by systematically changing the value of B_2^0 parameter. The IR and NIR data of **4** were fit using this model while allowing the other crystal field parameters to vary. As shown in Figure 6, varying B_2^0 has a large effect on the anisotropy of the EPR spectrum but only a minor effect on the average g-value. It is not possible to perform the same analysis for **3**, which has no site symmetry in the solid state. In this case, we note that the average g value for this complex, 1.15, is similar to the g-value of the highly symmetric uranium amide complex previously reported by Meyer, et al., 1.12,[52] so averaging the g-components produces a reasonable average value of g.

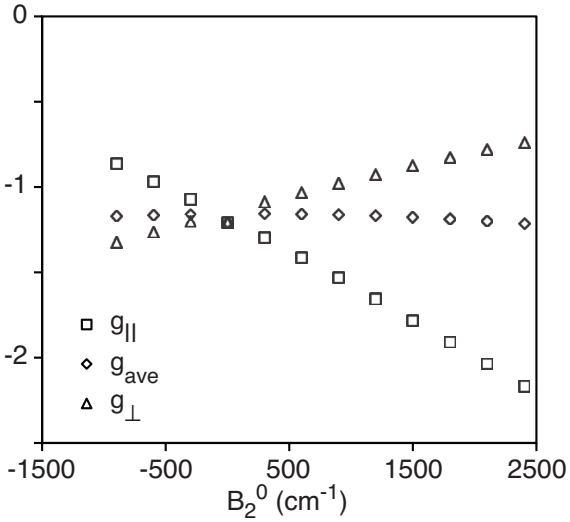

Figure 6. Effect of a trigonal distortion on the anisotropic and average g-values calculated using a CF model to fit the NIR spectrum $[U(NCR_2)_6]^-$ (**4**) and varying the value of B_2^0. The "dip" at $B_2^0 = 0$ is due to the fact that CF model does not perfectly model the spectrum of **4**.

Application of bonding models to f^1 complexes. The results of fitting the NIR and EPR data using the three models described above are shown in Table 2. The parameters for the fits are given in Table 3. In general, the fit parameters cannot be compared directly to previous studies as the models used are slightly different (except for the crystal field

model) and because the g-values, as well as the energies of the NIR transitions, are used in fitting.[17-20,38] The one exception is the work of Eichberger and Lux, who fit the f-f transitions and the g-values of a variety of f^1 hexahalide complexes using the Eisenstein and Pryce model, which is similar to the MO-T model.[19] The accuracy of the fits is best judged by comparing the experimental and calculated results in Table 2. Both the MO-RSO model and the MO-T model fit the data equally well in almost all cases. In some cases, the MO-T model fits the data exactly, which is not surprising since the number of parameters in the MO-T model is equal to the number of data. However, the MO-T model cannot be used to fit the data for the amide and alkyl complexes because it uses five parameters and only four data are available for these complexes. The relative precision of the models can be compared using the standard deviations of the derived parameters shown in Table 3. In most cases, the parameters are determined somewhat more precisely using the MO-RSO model than with the MO-T model, largely due to the fact that the MO-RSO model uses four parameters rather than the five parameters used in the MO-T model. In almost all cases, CF model is less precise than either MO model. As a result, the uncertainties in θ and Δ are typically larger for the CF model than for the MO-RSO or MO-T models. In addition, the fact that the CF model does not allow orbital reduction to differ for the different orbitals causes θ to be underestimated and Δ to be overestimated in comparison to the MO models. On the other hand, the CF model is excellent at modeling complexes with little covalency, as shown by the results for $CeCl_6^{3-}$ and $PaCl_6^{2-}$ where the CF model is arguably better than either MO model due to the smaller standard deviations of the fitting parameters. Likewise, the CF model is less accurate for complexes with significant covalency; the best example being UBr_6^-, which exhibits the largest covalency and the largest uncertainty in the CF parameters. The trend in covalency (α_π^2 and $\alpha_\pi'^2$) among the halide complexes is consistent with the intensities of the NIR transitions, which are strongest for the UBr_6^- and weakest for UF_6^-.

Table 2. Experimental NIR data and modeled results for octahedral f^1 complexes.[a]

	Model	Γ_8 (cm^{-1})	$\Gamma_{7'}$ (cm^{-1})	$\Gamma_{8'}$ (cm^{-1})	Γ_6 (cm^{-1})	g
$CeCl_6^{3-}$	Expt[53]	571	2161	2663	3050	-1.266
	MO-RSO	571	2166	2656	3053	-1.266
	MO-T	571	2161	2663	3050	-1.266
	CF	573	2161	2665	3048	-1.266
$PaCl_6^{2-}$	Expt[45,49]	2108	5250	7272	8173	-1.141
	MO-RSO	2156	5322	7115	8253	-1.141
	MO-T	2147	5251	7221	8207	-1.140
	CF	1984	5287	7105	8322	-1.138
UF_6^-	Expt[36,50,27]	5363	7400	13800	15900	-0.708
	MO-RSO	5398	7374	13773	15919	-0.708
	MO-T	5363	7400	13800	15900	-0.708
	CF	5111	7483	13438	16241	-0.701
UCl_6^-	Expt[36,48]	3800	6794	10137	11520	-1.12
	MO-RSO	3812	6791	10118	11533	-1.12
	MO-T	3800	6794	10137	11520	-1.12
	CF	3090	6764	9902	11916	-1.10
UBr_6^-	Expt[36,48]	3700	6830	9761	10706	-1.21
	MO-RSO	3731	6802	9712	10741	-1.21
	MO-T	3700	6830	9761	10706	-1.21
	CF	2705	6731	9419	11289	-1.19
$U(OR)_6^-$	Expt[32]	4873	7094	11221	13261	-0.73
	MO-RSO	4736	7129	11418	13137	-0.73
	MO-T	4807	7090	11221	13162	-0.73
	CF	4329	7116	11235	13414	-0.72
$U(NR_2)_6^-$	Expt[34]	--	6836	11181	13106	-1.15
	MO-RSO	3867	6836	11181	13106	-1.15
	MO-T[b]	--	--	--	--	--
	CF	3411	6884	10883	13325	-1.15
$U(NCR_2)_6^-$	Expt[35]	3240	6112	10234	12116	-1.22
	MO-RSO	3196	6134	10274	12089	-1.22
	MO-T	3240	6112	10234	12116	-1.22
	CF	3026	6137	10008	12339	-1.21
UR_6^-	Expt[31]	--	6832	10920	13436[c]	-1.43
	MO-RSO	2851	6928	10919	13436	-1.41
	MO-T[b]	--	--	--	--	--
	CF	2750	6832	10917	13666	-1.43
NpF_6	Expt[28,38,54]	7610	9355	24000	27000	-0.605
	MO-RSO	7661	9302	23984	27013	-0.606
	MO-T	7610	9355	24000	27000	-0.605
	CF	7466	9272	23343	27622	-0.596

a) Energies of the transitions for the halide complexes are taken from reference 19, except for those of $Cs_2NaCeCl_6$, which were taken from reference 53.
b) Too few data available to apply the MO-T model.
c) Error is estimated to be 1000 cm^{-1} rather than 100 cm^{-1}.

Table 3. Parameters obtained by fitting the NIR spectra of octahedral f^1 complexes.[a]

	Model	θ (10^3 cm^{-1})	Δ (10^3 cm^{-1})	α_σ^2	$\alpha_\pi'^2$	ζ_f (10^3 cm^{-1})[b]
$CeCl_6^{3-}$	MO-RSO	0.7(2)	0.36(8)	0.00(5)	0.02(6)	0.640
	MO-T	0.7(3)	0.4(2)	0.00(5)	0.01(7)	0.62(6)
	CF	0.7(1)	0.40(3)	--	--	0.63(3)
$PaCl_6^{2-}$	MO-RSO	2.6(4)	1.4(2)	0.04(4)	0.05(3)	1.621
	MO-T	4(1)	0.0(8)	0.3(3)	0.3(1)	1.7(1)
	CF	2.3(3)	1.53(9)	--	--	1.51(5)
UF_6^-	MO-RSO	7.7(1)	3.78(5)	0.13(2)	0.044(5)	2.085
	MO-T	7.8(2)	3.7(2)	0.26(7)	0.06(5)	2.04(7)
	CF	7.0(6)	4.0(3)	--	--	2.0(1)
UCl_6^-	MO-RSO	4.94(6)	1.81(4)	0.195(9)	0.054(6)	2.085
	MO-T	5.1(5)	1.6(4)	0.4(1)	0.07(6)	2.02(8)
	CF	4.1(8)	2.1(3)	--	--	1.9(2)
UBr_6^-	MO-RSO	5.0(2)	1.18(9)	0.27(3)	0.07(1)	2.085
	MO-T	5.4(4)	0.6(3)	0.9(2)	0.13(4)	2.1(1)
	CF	4(1)	1.7(5)	--	--	1.9(2)
$U(OR)_6^-$	MO-RSO	5.3(5)	3.5(2)	0.13(7)	0.06(2)	2.085
	MO-T	5.1(5)	3.7(3)	0.3(2)	0.00(9)	1.9(1)
	CF	4.7(6)	3.8(2)	--	--	1.9(1)
$U(NR_2)_6^-$	MO-RSO	6.2(2)	1.73(9)	0.14(4)	0.04(1)	2.085
	MO-T[c]	--	--	--	--	--
	CF	5.5(5)	1.9(2)	--	--	2.0(1)
$U(NCR_2)_6^-$	MO-RSO	6.2(2)	0.97(7)	0.12(2)	0.12(1)	2.085
	MO-T	6.1(3)	1.0(4)	0.19(7)	0.05(4)	1.81(6)
	CF	5.5(4)	1.4(2)	--	--	1.76(8)
UR_6^-	MO-RSO	6.8(5)	0.0(2)	0(2)	0.04(3)	2.085
	MO-T[c]	--	--	--	--	--
	CF	6.8(2)	0.00(9)	--	--	1.95(4)
NpF_6	MO-RSO	16.7(1)	5.22(7)	0.16(2)	0.042(6)	2.559
	MO-T	16.7(1)	5.1(1)	0.31(2)	0.06(1)	2.52(8)
	CF	16.1(8)	5.4(4)	--	--	2.4(2)

a) Standard deviations given in parentheses and are in the same units as the last digit of the parameter. Values without parentheses were not allowed to vary in the fit.

b) ζ_f in the case of the MO-RSO fit.

c) Too few data available to apply the MO-T model.

Modeling the NIR and EPR data produced two unexpected results. In almost all cases, the models generate very similar values of Δ and θ for any given complex. In other words, all of the models determine the magnitude of the ligand field with similar accuracy although the MO-RSO and MO-T models are more precise. The other surprising result is the effect of using reduced SO coupling constants, which is the primary difference between the MO-RSO and MO-T models. The main effect is that the covalency parameters, α_{σ}^2 and $\alpha_{\pi}'^2$, determined by the MO-RSO model are generally much smaller than those determined using the MO-T model. The reduced SO constants used in the MO-RSO include the same normalization constants as the orbital reduction parameters, so covalency has about twice the impact on SO coupling in the MO-RSO model relative to the MO-T model. Although the effect of covalency on the SO constant is partially accounted for in the MO-T model by allowing ζ to vary during fitting, covalency varies greatly among the orbitals (a_{2u} has no covalency, t_{1u} has some covalency, and t_{2u} is the most covalent).

Estimating the f orbital contribution to π and σ bonds from θ and Δ. As noted in the introduction, the primary goal of this study is to determine the strengths of individual π and σ bonds formed by the 5f orbitals. The parameters Δ and θ represent the destabilization of the metal-based antibonding f orbitals due to interactions with the ligands. Since the ligand orbitals are lower in energy than the metal orbitals, the stabilization of the filled ligand orbitals will be smaller than the destabilization of the f orbitals.[40] Using the Wolfsberg-Helmholz approximation,[55] the ratio of the stabilization of the bonding orbitals to the destabilization of the antibonding orbitals is $(E_X/E_M)^2$ to second order,[40,56] where E_M and E_X are the energies of the metal f orbitals and ligand orbitals, respectively (both the destabilization of the antibonding orbitals and the stabilization of the bonding orbitals are proportional to the square of the overlap, so the ratio does not depend on the overlap). The values of E_X may be obtained from the ionization potentials of the neutral ligands, which are known for the halogens,[57] and may be estimated for **1-4** from the ionization potentials of the neutral methyl,[58] hydroxyl,[59] and aminyl[60] radicals. The value of E_M may be estimated from the relevant atomic

ionization energies of the neutral metal atoms divided by the number of ionized electrons(e.g., the average ionization energy of U(V) is one fifth of the fifth ionization energy of atomic U).[61] The ionization energies of Ce are known,[57] and those of Np[62] and U[63] have been calculated. The fourth ionization potential of Pa was estimated by averaging the measured value for Th[57] and the calculated value for U.[63] Using this approach, the stabilization of the bonding orbitals, ΔE_{t1u} and ΔE_{t2u}, can be estimated from the destabilization of the antibonding orbitals as shown in eqns 2 and 3.

$$\Delta E_{t1u} \approx \left(\frac{E_M}{E_X}\right)^2 (\Delta + \theta) \quad (2)$$

$$\Delta E_{t2u} \approx \left(\frac{E_M}{E_X}\right)^2 \Delta \quad (3)$$

As shown by Burns and Axe, the group overlap for the t_{1u} orbital is equivalent to $(2)^{1/2}$ S_σ plus $(3/2)^{1/2}$ S_π, and the group overlap for the t_{2u} orbital is $(5/2)^{1/2}$ S_π.[25] In other words, the t_{1u} orbital participates in 2 σ and 1.5 π bonds, and the t_{2u} orbital forms 2.5 π bonds. Therefore, the strength of a single U-X σ bond is given by eqn 4 and that of a single U-X π bond is given by eqn 5, where the factor of 2 accounts for the presence of 2 electrons in each orbital. The average bond energy due to the interaction of the f orbital bonding (including both σ and π bonding) is $\Delta E_{t1u} + \Delta E_{t2u}$. The previously estimated π and σ bond strengths in UF_6^-, UCl_6^-, UBr_6^- and **4** were not corrected for the differences between the ligand and metal orbital energies and were too small by a factor of two.[35] These effects roughly cancel resulting in values similar to those determined here.

$$E_\pi = 2\left(\frac{2}{5}\Delta E_{t1u}\right) \quad (4)$$

$$E_\sigma = 2\left(\frac{1}{2}\Delta E_{t2u} - \frac{3}{10}\Delta E_{t1u}\right) \quad (5)$$

Equations 4 and 5 are based on the assumption that each ligand possesses two p orbitals that act as π donors towards the metal center, which is the case in the halide and alkoxide complexes. In contrast, **3** and **4** have only a single p orbital capable of acting as a

π donor, so the value of E_π given in eqn 4 must be doubled to determine the strength of a single π bond.

In the MO models, the electron density on the f-orbitals in the bonding orbitals is equal to the electron density on the ligands in the antibonding orbitals. The normalized covalency in the t_{2u} orbital is $N'^2\alpha_\pi'^2$, and the normalized covalency in the t_{1u} orbital is $N^2[\alpha_\sigma^2 + (3/5)\,\alpha_\pi'^2]$. The strengths of the U-X σ and π interactions along with the normalized covalency in the bonding t_{1u} and t_{2u} orbitals are given in Table 4. The estimated bond energies are not strongly affected by the choice of the Wolfsberg-Helmholz approximation; using the Ballhausen-Gray approximation produces very similar results (Table S3).

Table 4. Covalency in the bonding t_{1u} and t_{2u} orbitals and estimated strengths of bonds formed between the ligands and the f orbitals. (Avg M-X is the contribution of only f orbital bonding to the bond strength)

Complex E (eV)	Model	% f-orbital e$^-$ density[a] $t_{1u}(\sigma,\pi)$	$t_{2u}(\pi)$	σ bond (kcal mol^{-1})	π bond[b] (kcal mole^{-1})	Avg M-X (kcal mole^{-1})
$CeCl_6^{3-}$	MO-RSO	1(8)	2(6)	0.7	0.2	1.1
E_M=6.73	MO-T	0(8)	1(6)	0.6	0.2	1.1
E_X=12.97	CF	--	--	0.6	0.2	1.1
$PaCl_6^{2-}$	MO-RSO	6(5)	5(3)	3.0	1.1	5.2
E_M=7.60	MO-T	31(26)	22(9)	4.0	0.0	4.0
E_X=12.97	CF	--	--	2.8	1.2	5.2
UF_6^-	MO-RSO	14(2)	4.2(5)	7.6	2.5	12.5
E_M=9.33	MO-T	23(8)	6(4)	7.6	2.4	12.4
E_X=17.42	CF	--	--	7.1	2.6	12.4
UCl_6^-	MO-RSO	19(1)	5.1(6)	8.4	2.1	12.7
E_M=9.33	MO-T	30(10)	7(6)	8.5	1.8	12.2
E_X=12.97	CF	--	--	7.3	2.5	12.4
UBr_6^-	MO-RSO	24(3)	7(1)	9.8	1.7	13.1
E_M=9.33	MO-T	50(20)	12(4)	10.1	0.8	11.7
E_X=11.81	CF	--	--	7.8	2.4	12.7
$U(OR)_6^-$	MO-RSO	14(8)	6(2)	9.8	4.2	18.1
E_M=9.33	MO-T	20(20)	0(8)	9.6	4.4	18.4
E_X=13.02	CF	--	--	9.1	4.4	18.0
$U(NR_2)_6^-$	MO-RSO	14(5)	4(1)	13.0	5.3	18.3
E_M=9.33	MO-T[c]	--	--	--	--	--
E_X=11.46	CF	--	--	11.8	5.8	17.7
$U(NCR_2)_6^-$	MO-RSO	16(3)	10(1)	12.5	2.9	15.5
E_M=9.33	MO-T	19(8)	5(4)	12.4	3.1	15.5
E_X=11.46	CF	--	--	11.4	4.3	15.8
UR_6^-	MO-RSO	5(70)	3(3)	17.5	0.0	17.5
E_M=9.33	MO-T[c]	--	--	--	--	--
E_X=9.84	CF	--	--	17.6	0.0	17.6
NpF_6	MO-RSO	16(3)	4.1(5)	20.9	4.6	30.2
E_M=10.87	MO-T	26(3)	5.8(5)	20.9	4.5	30.0
E_X=17.42	CF	--	--	20.4	4.8	30.0

a) Fraction of the electron density that resides on the metal f-orbitals in the bonding orbitals; the standard deviation is given in parentheses

b) Note that the strength of a π bond is doubled for $U(NR_2)_6^-$ and $U(NCR_2)_6^-$ since the complexes contain half of the 5f p π donor interactions of the other complexes.

c) Too few data to apply the MO-T model.

The contribution of f orbital bonding to the total bond energy may be examined for the halide complexes. The average bond dissociation energy (BDE) for NpF_6 is 113 kcal mol^{-1},[64] so 5f orbital bonding (Avg M-X in Table 4) is responsible for approximately one quarter of the bond strength. The proportion of the BDE due to f orbital bonding in NpF_6 seems quite high, and it should be noted that the energies assigned to the Γ_8' and Γ_6 states in this complex have been questioned.[20,38] Relativistic calculations for UF_6 show that 5f orbital bonding is responsible for ~25% of the BDE, which supports both the energy assignments and the proportion of BDE due to f orbital bonding in NpF_6.[65] While the BDEs of the other complexes have not been reported, those of UF_5, UCl_5, and UBr_5 are 137,[66] 99,[67] and 84 kcal mol^{-1},[68] respectively. Assuming that the BDEs of the uranium hexahalide anions are similar, f orbital bonding is responsible for 10% of the average BDE in UF_6^- and 20% of the average BDE in UBr_6^-. Despite the increased covalency in UBr_6^-, the bonding in UF_6^- is much stronger, presumably due to the greater ionic stabilization afforded by the short U-F bond as well as the contributions of the U 6d orbitals to bonding.[69]

The most interesting ligand studied here is the ketimide ligand. As shown in Table 4, the strength of the 5f σ bond of the ketimide ligand is essentially the same as that of the amide ligand. However, Table 4 suggests that ketimide is a much weaker π donor than the amide ligand. This interpretation is strongly contradicted by efficacy of ketimide ligands for stabilizing highly oxidized metal centers, which indicates that ketimide is a strong π donor.[70-72] The reduction potentials of pentavalent organouranium complexes also show that ketimide is a strong π donor.[73] This apparent contradiction can be understood by noting that ketimide is also a π acceptor due to the presence of a low-lying CN π^*-orbital.[70,74] Since the model used here assumes octahedral symmetry, the value of Δ reflects the effects of both the π donating and π accepting ketimide 2p orbitals. The π accepting orbital of the ketimide ligand decreases Δ, which makes ketimide seem like a weaker π donor than the amide. The presence of the π back bonding between the 5f orbitals and the ketimide π acceptor orbital should increase the ligand character in the t_{2u} orbital relative to that of the amide ligand, which is consistent with the increased

π covalency shown in Table 4. The increased covalency of the U-ketimide bond relative to the U-amide bond is consistent with previous studies of bonding of $Cp^*_2UX_2$ ($Cp^* = C_5Me_5$; X = amide, ketimide), in which a large increase in the intensities of the f transitions in the ketimide complex relative to the amide complex was attributed to an intensity stealing mechanism due to greater covalency in the uranium ketimide bond.[75]

Covalency in 5f ligand bonding. As noted above, one of the surprising results of this study is the difference in covalency between the MO-RSO and MO-T models. Because it uses reduced SO coupling, the MO-RSO model predicts less covalency in 5f ligand bonds than the MO-T model, especially for σ bonding. Ideally, one would like to compare the amount of ligand character in the models to experimental measurements of covalency; however, NpF_6 is the only octahedral f^1 complex for which the covalency has been reported. Since ENDOR results were used to calibrate the ζ_f for the MO-RSO model, we cannot use them to compare the MO-RSO and MO-T models.[28] The only other relevant experimental result is the covalency in UCl_6^{2-}, which was determined using XAS spectroscopy.[2] The total ligand covalency in the t_{1u} and t_{2u} orbitals in UCl_6^{2-} is 0.087 after converting from the covalency per bond to the covalency per orbital. This data may be compared to the covalency in the only tetravalent ion studied here, $PaCl_6^{2-}$. The total covalency in $PaCl_6^{2-}$ for the MO-RSO and MO-T models is 0.11 and 0.40, respectively; as determined by the sum of the ligand character in the t_{1u} and t_{2u} orbitals. The errors are, however, very large for this complex. While the comparisons are not direct, the covalency of the f-orbital bonds determined using the MO-RSO model are similar to that determined by X-ray absorption spectroscopy for other actinide complexes, and the covalency determined using the MO-T mode is significantly greater.[76,77]

Few computational results are available for comparison with the covalency in the two MO models, despite the fact that these complexes have been extensively studied using computational techniques. Some octahedral f^1 ions have been studied using Xα calculations and self-consistent field Dirac scattered wave (DSW) calculations.[21,29,30,78] The results of these calculations are compared with the results from the MO-RSO and MO-T model in Table 5. In the case of UF_6^-, there is good quantitative agreement

between the MO-RSO model and the Xα and DSW calculations for the orbitals involved in σ antibonding (Γ_6 and Γ_8') and poor agreement between the calculations for the MO-T model.[21,29,30,78] There is similarly good agreement between the MO-RSO model and the covalency in the bonding orbitals of UF_6^- determined using Xα calculations. For $PaCl_6^{2-}$, there is qualitative agreement between the MO-RSO model and the DSW calculation for the σ antibonding orbitals and poor agreement with the MO-T model. For the π antibonding orbitals, there is qualitative agreement between both models and both calculations for UF_6^- and NpF_6, but the MO-T results for $PaCl_6^{2-}$ are in poor agreement. The bonding in NpF_6 has studied recently using relativistically corrected density functional theory.[79] In this case, the degree of covalency in the Np-F bond, 16%, is in good agreement with that of the σ bond in the MO-RSO model, but not in good agreement with that predicted by the MO-T model. The amount of covalency determined using the MO-T is much greater than the calculations. This result underscores the role of reduced SO coupling in the MO-RSO model, which results in much less covalency in comparison to the MO-T model.

Table 5. Ligand character (%) in the antibonding orbitals of UF_6^-, $PaCl_6^{2-}$, and NpF_6

Complex	Orbital	MO-RSO	MO-T	Xα[21]	DSW[29,30,78]
UF_6^-	Γ_6	13.8	23.0	14.1	15.2
UF_6^-	Γ_8'	12.6	21.2	13.6	16.9
UF_6^-	Γ_7'	3.0	4.1	5.6	4.4
UF_6^-	Γ_8	5.6	8.4	11.9	9.7
UF_6^-	Γ_7	1.3	1.9	3.8	3.2
$PaCl_6^-$	Γ_6	6.5	31.1		10.3
$PaCl_6^-$	Γ_8'	5.8	29.5		8.5
$PaCl_6^-$	Γ_7'	2.6	11.2		6.3
$PaCl_6^-$	Γ_8	5.3	23.7		8.8
$PaCl_6^-$	Γ_7	2.1	13.2		2.7
NpF_6	Γ_7	1.2	1.7		0.9

The alkyl complex, **1**, has also been studied by computationally.[31] In this case, only the results for the occupied, bonding orbitals have been reported and are calculated to possess significant 5f character.[31] While the MO-RSO model does predict that **1** does possess some covalency in the σ bond between U and the alkyl ligand, the uncertainty in the

energy of the Γ_6 orbital produces a large uncertainty in the covalency making a direct comparison with theory impossible.

The limited amount of experimental and computational data suggests that the MO-T model overestimates the amount of covalency in the M-X bonds. Since the MO-T model is not widely used, this may seem irrelevant. However, the MO-T model is very similar to the more widely used Eisenstein and Pryce model.[37,38] These results show that the orbital reduction parameters in the Eisenstein and Pryce model, k and k', are much larger than one would expect based solely on orbital reduction. As a result, estimates of covalency based solely on k and k' may overestimate the amount of covalency in actinide-ligand bonds.

The results in Table 4 also reveal that the correlation between covalency and the strength of f orbital bonding is not straightforward, which has been addressed previously by Notter and Bolvin, in somewhat different manner than that used here.[22] First order bonding theory has also been used to explain these trends.[1,2] The results in Table 4 can be understood in a similar manner using second order theory previously applied to transition metal complexes by Burdett.[56] Using a second order model and the Wolfsberg-Helmholz approximation,[55] the stabilization of the bonding orbital, ΔE, and the unnormalized electron density that resides on the metal center, α^2, may be approximated by eqn 6 and 7.[56] Note that α^2 is the unnormalized covalency used in Scheme 1, but the subscript has been removed to show that these are general relationships (e.g., the stabilization of the ligand t_{2u} orbital due to π bonding is ΔE_{t2u} and the unnormalized covalency is $\alpha_{\pi}'^2$). The main difference between the eqn 6 and 7 is that the denominator in eqn 7 is squared. As a result, covalency has a much stronger dependence on the orbital energies than the bond strength as previously noted by both experimental and computational studies.[1,7,8]

$$\Delta E \approx \frac{|SE_M|^2}{(E_M - E_X)} \tag{6}$$

$$\alpha^2 \approx \frac{S^2 E_M E_X}{(E_M - E_X)^2} \tag{7}$$

A number of interesting trends can be seen in Table 4. The most notable trend is the relationship between the oxidation state and the strength of f-orbital bonding. The bond energies vary somewhat within a given oxidation state, but they vary greatly between oxidation states: 1 kcal mol^{-1} for Ce(III), 5 kcal mol^{-1} for Pa(IV) to 12 to 18 kcal mol^{-1} for U(V), and 30 kcal mol^{-1} for Np(VI). Both the limited variation in bond strengths within an oxidation state and the large variation between oxidation states may be explained by changes in E_X and E_M. As the oxidation state increases, the metal orbitals become lower in energy, so the numerator in eqn 6 increases greatly and the denominator decreases resulting in stronger bonding as well as increased covalency. The effect is magnified for $CeCl_6^-$ since the overlap is smaller for this complex. In comparison, varying the ligand has a relatively minor effect on the bond energies since the impact is largely limited to the denominator.

The framework described in eqns 6 and 7 explains the changes in covalency and bond strength as the ligands are varied. In the U(V) halide complexes, covalency increases dramatically from UF_6^- through UBr_6^-, yet the σ bond strength varies only slightly. As one moves down the halogen group, the numerators of eqns 6 and 7 and (E_M-E_X) decrease as the ligand orbitals become less stable and the bond lengths increase, which presumably decreases S. Since the value of $(E_M-E_X)^2$ decreases more rapidly than does the value of (E_M-E_X), the amount of covalency increases more quickly than does the bond strength. A similar trend in σ bond energies is observed among **1-4** along with UF_6^-. As one moves across the first-row ligands from alkyl through fluoride, E_M-E_X increases, and the strength of U-X σ bond decreases as expected. Only a small change in covalency is expected in this case because S should change only slightly among these orbitals, so both the numerator and denominator in eqn 7 increase as one proceeds from **1** through UF_6.

On the whole, an increase in f orbital covalency results in an increase in strength of the resulting f orbital bond although the relationship is clearly not linear. However, increased f orbital covalency does not imply an increase in BDE since f orbital bonding is not a major contributor to the overall bond strength. In addition, the overlap between the

ligands and the d orbitals is larger than the f orbital overlap, and d orbital bonding may result in stronger bonding despite the lower stability of these orbitals.[69] Consequently, even though the covalency and strength of the bond formed between the ligand and the uranium f orbitals in UBr_6^- are greater than in UF_6^-, UF_6^- certainly has a greater BDE than does UBr_6^-. This situation is reminiscent of the "FEUDAL" (f's essentially unaffected, d's accommodate ligands) model described by Bursten and coworkers in that f orbital bonding is never the major contributor the BDE.[40] However, when the energy of the f orbitals approaches that of the ligand orbitals, as in UX_6^- and NpF_6, the f orbitals are no longer unaffected by interaction with the ligand orbitals.

Conclusions

The MO-T model for bonding in f^1 ions described by Thornley was extended to form an new model (MO-RSO), which includes the effect of covalency on SO coupling in addition to the effect of covalency on orbital reduction. To apply the MO-RSO model to the data available for octahedral f^1 ions, it was simplified by using hybrid sp σ bonding orbitals on the ligands and by expressing the covalency introduced by π bonding in the t_{1u} orbital, α_π^2, in terms of the covalency in the t_{2u} orbital, $\alpha_\pi'^2$; neither of these simplifications affects its accuracy. The main assumption that is necessary to apply either MO model to the data is that overlap between the f orbitals and the ligand orbitals is small compared with covalency and may be ignored.

The MO-T, MO-RSO and the CF models were applied to the spectroscopic data of a variety of octahedral f^1 complexes to determine the strength and covalency of the π and σ bonds formed by the f orbitals. When covalent bonding is significant, MO models are more precise; however, when covalent bonding is not strong, the CF model worked better. The covalency determined using the MO-RSO model is in better agreement with experiment and theory than that predicted by the MO-T model.

The stabilization of the bonding orbitals was estimated from the destabilization of the antibonding orbitals using the energies of the ligand and metal orbitals. The resulting bond energies are much smaller than the destabilization of the antibonding orbitals and

largely reflect the energies of the metal orbitals: stronger, more covalent bonds are formed as the metal oxidation state increases. The trends in both bond strength and covalency can be understood using the second-order framework previously used by Burdett for transition metal complexes. The strength of the bonds formed between the ligands and f orbitals are relatively small compared with the total bond dissociation energy.

Experimental

General. All solvents were dried over and distilled from sodium benzophenone ketyl. Glassware was oven dried for at least 24 hr prior to use. All manipulations were carried out in an argon-filled glove box. Complexes **1**-**4** were prepared as previously reported.[31-35]

EPR spectroscopy. Samples were finely powered and sealed in quartz EPR tubes under argon. Spectra were recorded on a Varian E-12 Century spectrometer equipped with an AIP frequency counter and Varian Gaussmeter previously calibrated using DPPH in the sample cavity. Simulations were performed using a version of the code ABVG that has been modified to perform least squares fitting.[80]

Magnetic Susceptibility of $[Li(OEt_2)][U(O^tBu)]_6$ (2). Sample was sealed in 2 mm quartz tubing between two plugs of quartz wool. Susceptibility was corrected for inherent diamagnetism of the complexes using Pascal's constants. The magnetization of **2** was corrected for the presence of a ferromagnetic impurity using data taken at 0.5 T and 1 T; the fact that the susceptibility of a ferromagnet is field and temperature independent; and eq 13 where $M_{sample}(T)$ and $M_{measured}(T)$ are the magnetization of the sample and measured magnetization, respectively, and M_{ferro} is the magnetization of the ferromagnetic impurity, which is field and temperature independent. The magnetization due to the ferromagnetic impurity is similar to that from the sample due to the small magnetic moment of U(V).

$$M_{sample}(T)=M_{measured}(T) - M_{ferro} \qquad (13)$$

To obtain the value of χT at 0 K, data were plotted as vs. T, and the value of χT was extrapolated to 0 K. The value of χT at 0 K is unaffected by the ferromagnetic correction.

NIR Spectra. Samples were dissolved in THF in the glove box and placed in 10 mm cuvettes with a septum, screw-cap seal. Data were obtained using a Cary 5G spectrometer. The spectrum of the alkyl complex, **2**, was fit using pseudo-Voigt peaks as shown in Figure S2 to obtain the energies of the NIR transitions.

Data fitting. All calculations for the octahedral models done using Microsoft Excel. All fits to the models were performed by minimizing $\Sigma(\text{experiment-model})^2/(\text{uncertainty})^2$, where the uncertainty in the EPR measurements was assumed to be 0.01 and the uncertainty in the NIR measurements was assumed to be 100 cm^{-1} except for the energy of the Γ_6 transition in $[UR_6]^-$, **1**, for which the error was assumed to be 1000 cm^{-1}. Standard deviations were determined by first normalizing chi-squared to the degrees of freedom in the fit. When the degrees of freedom were zero, chi-squared was normalized to 0.5 if it was greater than this value and was not changed if less than this value. Following normalization of chi-squared, the standard deviation was determined by changing the value of one parameter and allowing the other parameters to vary to minimize chi-squared until the value of chi-squared increased by one.

Acknowledgement

We thank Stefan Minasian, Richard Martin, Nikolas Kaltsoyannis, and Jorgen Ausbach for helpful discussions. Work at UCSB was supported by the U.S. Department of Energy, Office of Basic Energy Sciences, Chemical Sciences, Biosciences, and Geosciences Division under Contract No. DE-FG02-09ER16067. Portions of this work were supported by U.S. Department of Energy, Basic Energy Sciences, Chemical Sciences, Biosciences, and Geosciences Division and were performed at Lawrence Berkeley National Laboratory under Contract No. DE-AC02-05CH11231.

Associated Content

Supporting Information

Mixing of the a_{2u}, t_{1u}, and t_{2u} orbitals in an octahedral f^1 complex. Magnetic susceptibility of $[Li(Et_2O)[U(O^tBu)_6]$, **2**. NIR spectra and fitted models for **1-4**. % Ligand character in the f-orbitals in the MO models. Covalency and bond strengths estimated using the Ballhausen-Gray model. Derivation of eq 7. This material is available free of charge via the Internet at http://pubs.acs.org.

References

(1) Neidig, M. L.; Clark, D. L.; Martin, R. L. *Coord. Chem. Rev.* **2013**, *257*, 394.
(2) Minasian, S. G.; Keith, J. M.; Batista, E. R.; Boland, K. S.; Clark, D. L.; Conradson, S. D.; Kozimor, S. A.; Martin, R. L.; Schwarz, D. E.; Shuh, D. K.; Wagner, G. L.; Wilkerson, M. P.; Wolfsberg, L. E.; Yang, P. *J. Am. Chem. Soc.* **2012**, *134*, 5586.
(3) Liu, G. K. *J. Solid State Chem.* **2005**, *178*, 489.
(4) Batista, E. R.; Martin, R. L.; Hay, P. J. *J. Chem. Phys.* **2004**, *121*, 11104.
(5) Batista, E. R.; Martin, R. L.; Hay, P. J.; Peralta, J. E.; Scuseria, G. E. *J. Chem. Phys.* **2004**, *121*, 2144.
(6) Barros, N.; Maynau, D.; Maron, L.; Eisenstein, O.; Zi, G.; Andersen, R. A. *Organometallics* **2007**, *26*, 5059.
(7) Tassell, M. J.; Kaltsoyannis, N. *Dalton Trans.* **2010**, *39*, 6719.
(8) Kirker, I.; Kaltsoyannis, N. *Dalton Trans.* **2011**, *40*, 124.
(9) Choppin, G. R.; Jensen, M. P. In *The Chemistry of the Actinide Elements*; Morss, L., Edelstein, N. M., Fuger, J., Eds.; Springer: Berlin, 2006; Vol. 3.
(10) Gaunt, A. J.; Reilley, S. D.; Enriquez, A. E.; Scott, B. L.; Ibers, J. A.; Sekar, P.; Ingram, K. I. M.; Kaltsoyannis, N.; Neu, M. P. *Inorg. Chem.* **2008**, *47*, 29.
(11) Jensen, M. P.; Bond, A. H. *J. Am. Chem. Soc.* **2002**, *124*, 9870.
(12) Mazzanti, M.; Wietzke, R.; Pecaut, J.; Latour, J.-M.; Maldivi, P.; Remy, M. *Inorg. Chem.* **2002**, *41*, 2389.
(13) Berthet, J.-C.; Miquel, Y.; Iveson, P. B.; Nierlich, M.; Thuery, P.; Madic, C.; Ephritikhine, M. *Dalton Trans.* **2002**, 3265.
(14) Kolarik, Z.; Mullich, U.; Gassner, F. *Solv. Extr. Ion Exch.* **1999**, *17*, 23.
(15) Shannon, R. D. *Acta Cryst.* **1976**, *A32*, 751.
(16) Strittmatter, R. J.; Bursten, B. E. *J. Am. Chem. Soc.* **1991**, *113*, 552.
(17) Edelstein, N. *Rev. Chim. Miner.* **1977**, *14*, 149.
(18) Edelstein, N.; Brown, D.; Whittaker, B. *Inorg. Chem.* **1974**, *13*, 563.
(19) Eichberger, K.; Lux, F. *Ber. Bunsenges. Phys. Chem.* **1980**, *84*, 800.
(20) Hecht, H. G.; Burton Lewis, W.; Eastman, M. P. *Adv. Chem. Phys.* **1969**, *16*, 351.
(21) Kaltsoyannis, N.; Bursten, B. E. *Inorg. Chem.* **1995**, *34*, 2735.
(22) Notter, F.-P.; Bolvin, H. *J. Chem. Phys.* **2009**, *130*, 184310.
(23) Ohwada, K. *J. Inorg. Nucl. Chem.* **1976**, *38*, 741.
(24) Owen, J.; Thornley, T. H. M. *Rep. Prog. Phys.* **1966**, *29*, 675.
(25) Burns, G.; Axe, J. D. In *Optical Properties of Ions in Crystals*; Chrosswhite, H. M., Moos, H. W., Eds.; Interscience: New York, 1967.

(26) Kozimor, S. A.; Yang, P.; Batista, E. R.; Boland, K. S.; Burns, C. J.; Clark, D. L.; Conradson, S. D.; Martin, R. L.; Wilkerson, M. P.; Wolfsberg, L. E. *J. Am. Chem. Soc.* **2009**, *131*, 12125.
(27) Reisfeld, M. J.; Crosby, G. A. *Inorg. Chem.* **1965**, *4*, 65.
(28) Butler, J. E.; Hutchison, C. A. *J. Chem. Phys.* **1981**, *74*, 3102.
(29) Arratia-Pérez, R.; Malli, G. L. *J. Chem. Phys.* **2006**, *124*, 074321.
(30) Arratia-Pérez, R.; Hernandez-Acevedo, L.; Malli, G. L. *J. Chem. Phys.* **2004**, *121*, 7743.
(31) Fortier, S.; Walensky, J. R.; Wu, G.; Hayton, T. W. *J. Am. Chem. Soc.* **2011**, *133*, 11732.
(32) Fortier, S.; Wu, G.; Hayton, T. W. *Inorg. Chem.* **2008**, *47*, 4752.
(33) Fortier, S.; Wu, G.; Hayton, T. W. *Inorg. Chem.* **2009**, *48*, 3000.
(34) Seaman, L. A.; Fortier, S.; Wu, G.; Hayton, T. W. *Inorg. Chem.* **2011**, *50*, 636.
(35) Seaman, L. A.; Wu, G.; Edelstein, N.; Lukens, W. W.; Magnani, N.; Hayton, T. W. *J. Am. Chem. Soc.* **2012**, *134*, 4931.
(36) Ryan, J. L. *J. Inorg. Nucl. Chem.* **1971**, *33*, 153.
(37) Thornley, T. H. M. *Proc. Phys. Soc.* **1966**, *88*, 325.
(38) Eisenstein, J. C.; Pryce, M. H. L. *Proc. R. Soc. Lond. A* **1960**, *255*, 181.
(39) Stevens, K. W. H. *Proc. R. Soc. Lond. A* **1953**, *219*, 542.
(40) Albright, T. A.; Burdett, J. K.; Whangbo, M.-H. *Orbital Interactions in Chemistry*; John Wiley & Sons: New York, 1985.
(41) Misetich, A. A.; Buch, T. *J. Chem. Phys.* **1964**, *41*, 2524.
(42) Misetich, A. A.; Watson, R. E. *Phys. Rev.* **1966**, *143*, 335.
(43) Kramida, A.; Raichenko, Y.; Reader, J.; NIST ASD Team, "NIST Atomic Spectra Database (ver. 5.0)" **2012**, National Institute of Standards and Technology, Gaithersburg, MD.
(44) Lewis, W. B.; Mann, J. B.; Liberman, D. A.; Cromer, D. T. *J. Chem. Phys.* **1970**, *53*, 809.
(45) Piehler, D.; Kot, W. K.; Edelstein, N. *J. Chem. Phys.* **1991**, *94*, 942.
(46) Lever, A. B. P. *Inorganic Electronic Spectroscopy (Second Edition)*; Elsevier: Amsterdam, 1984.
(47) Rosenzweig, A.; Cromer, D. T. *Acta Cryst.* **1967**, *23*, 865.
(48) Selbin, J.; Sherrill, H. J. *Inorg. Chem.* **1974**, *13*, 1235.
(49) Axe, J. D.; Stapleton, H. J.; Jeffries, C. D. *Phys. Rev.* **1961**, *121*, 1630.
(50) Rigny, P.; Dianoux, A. J.; Plurien, P. *J. Phys. Chem. Solids* **1971**, *32*, 1175.
(51) Baker, J. M.; Davies, E. R. *J. Phys. C.: Solid State Phys.* **1975**, *8*, 1869.
(52) Meyer, K.; Mindiola, D. J.; Baker, T. A.; Davis, W. M.; Cummins, C. C. *Angew. Chem. Int. Ed.* **2000**, *39*, 3063.
(53) Tanner, P. A.; Mak, C. S. K.; Edelstein, N. M.; Murdoch, K. M.; Liu, G.; Huang, J.; Seijo, L.; Barandiaran, Z. *J. Am. Chem. Soc.* **2003**, *125*, 13225.
(54) Mulford, R. N.; Dewey, H. J.; Bareflield, J. E. *J. Chem. Phys.* **1991**, *94*, 4790.
(55) Wolfsberg, M.; Helmholz, L. *J. Chem. Phys.* **1952**, *29*, 837.
(56) Burdett, J. K. *J. Am. Chem. Soc.* **1979**, *101*, 580.
(57) Moore, C. E. *Ionization potentials and ionization limits derived from the analyses of optical spectra*, National Bureau of Standards, 1970.
(58) Houle, F. A.; Beauchamp, J. L. *J. Am. Chem. Soc.* **1979**, *101*, 4067.

(59) Wiedmann, R. T.; Tonkyn, R. G.; White, M. G.; K., W.; McKoy, V. *J. Chem. Phys.* **1992**, *97*, 768.
(60) Gibson, S.; Green, J. C.; Berkowitz, J. *J. Chem. Phys.* **1985**, *83*, 4319.
(61) DeKock, R. L.; Gray, H. B. *Chemical Structure and Bonding*; Benjamin/Cummings: Menlo Park, 1980.
(62) Zhou, W. D.; Dong, C. Z.; Wang, Q. M.; Wang, X. L.; Saber, I. A. *Eur. Phys. J. D* **2012**, *66*, 260.
(63) Rashid, K.; Saadi, M. Z.; Yasin, M. *At. Data Nucl. Data Tables* **1988**, *40*, 365.
(64) Galkin, N. P.; Tumanov, Y. N. *Russ. Chem. Rev.* **1971**, *40*, 154.
(65) Straka, M.; Patzschke, M.; Pykko, P. *Theor. Chem. Acc.* **2003**, *109*.
(66) Hildenbrand, D. L.; Lau, K. H. *J. Chem. Phys.* **1991**, *94*, 1420.
(67) Lau, K. H.; Hildenbrand, D. L. *J. Chem. Phys.* **1984**, *80*, 1312.
(68) Lau, K. H.; Hildenbrand, D. L. *J. Chem. Phys.* **1987**, *86*, 2949.
(69) Bursten, B. E.; Strittmatter, R. J. *Angew. Chem. Int. Ed.* **1991**, *30*, 1069.
(70) Soriaga, R. A. D.; Nguyen, J. M.; Albright, T. A.; Hoffmann, D. M. *J. Am. Chem. Soc.* **2010**, *132*, 18014.
(71) Lewis, R. A.; Guang, W.; Hayton, T. W. *Inorg. Chem.* **2011**, *50*, 4660.
(72) Lewis, R. A.; Guang, W.; Hayton, T. W. *J. Am. Chem. Soc.* **2010**, *132*, 12814.
(73) Graves, C. R.; Vaughn, A. E.; Schelter, E. J.; Scott, B. L.; Thompson, J. D.; Morris, D. E.; Kiplinger, J. L. *Inorg. Chem.* **2008**, *47*, 11879.
(74) Clark, A. E.; Martin, R. L.; Hay, P. J.; Green, J. C.; Jantunen, K. C.; Kiplinger, J. L. *J. Phys. Chem. A* **2005**, *109*, 5481.
(75) Morris, D. E.; Da Re, R. E.; Jantunen, K. C.; Castro-Rodriguez, I.; Kiplinger, J. L. *Organometallics* **2004**, *23*, 5142.
(76) Spencer, L. P.; Yang, P.; Minasian, S. G.; Jilek, R. E.; Batista, E. R.; Boland, K. S.; Boncella, J. M.; Conradson, S. D.; Clark, D. L.; Hayton, T. W.; Kozimor, S. A.; Martin, R. L.; MacInnes, M. M.; Olson, A. C.; Scott, B. L.; Shuh, D. K.; Wilkerson, M. P. *J. Am. Chem. Soc.* **2013**, *135*, 2279.
(77) Kozimor, S. A.; Yang, P.; Batista, E. R.; Boland, K. S.; Burns, C. J.; Clark, D. L.; Conradson, S. D.; Martin, R. L.; Wilkerson, M. P.; Wolfsberg, L. E. *J. Am. Chem. Soc.* **2009**, *131*, 12125.
(78) Case, D. A. *J. Chem. Phys.* **1985**, *83*, 5792.
(79) Aquino, F.; Pritchard, B.; Autschbach, J. *J. CHem. TheoryComput.* **2012**, *8*, 598.
(80) Daul, C.; Schlapfer, C. W.; Mohos, B.; Ammeter, J.; Gamp, E. *Comput. Phys. Commun.* **1981**, *21*, 385.

TOC Figure (encapsulated postscript file)